Nonequilibrium distribution functions for general rigid bodies in axially symmetric environments

M. Thachuk
Chemistry Department, University of British Columbia, Vancouver, Canada V6T 1Z1
(Received 30 June 2005; published 21 September 2005)

A vector $\boldsymbol{\rho}$ is introduced in such a manner that the equilibrium rotational distribution function for a general rigid body has a simple quadratic form both from a body-fixed and space-fixed frame of reference. It is shown that when considering nonequilibrium distribution functions, representations employing the components of $\boldsymbol{\rho}$ generalize more easily than those employing the components of the angular momentum or angular velocity, and lead to forms with greater accuracy. The behavior of $\boldsymbol{\rho}$ and its relation to the angular momentum of the system is explored in some detail. Comparisons are made with distribution functions generated from molecular dynamics simulations of H_2O^+ drifting in a helium bath gas under the influence of a uniform electric field.

DOI: 10.1103/PhysRevA.72.032722 PACS number(s): 34.10.+x

I. INTRODUCTION

There are many physical scenarios in which particles move in an axially symmetric environment. In the present case, motivation was provided by ion mobility experiments, in which ions drift in a bath gas under the influence of a constant, external electric field [1]. The distribution function for the drifting ions is axially symmetric about the field direction, even in the nonequilibrium situation when the field strength is large. A similar situation exists in a molecular beam expansion, in which seed molecules are subjected to the unidirectional slip velocity of an expanding bath gas [2–6]. Injecting ions with large momenta along a fixed axis into a thermalized bath gas also produces an axially symmetric environment along the injection axis [7,8]. In fact, any experiment in which particles move through a gas preferentially in one direction will produce similar distributions.

As a specific case, mobility experiments will be considered from this point onwards, although the results generalize beyond this limit. In a mobility experiment, the distribution function is typically expressed as a function of the velocity and angular momentum of the ion, that is $f(\mathbf{v},\mathbf{J})$, and we are interested in describing this function in the space-fixed (SF) frame. This frame is synonymous with the lab frame in which the experiment is performed, and in which a constant, uniform electric field is produced. Define the SF frame z axis to lie along the electric field direction.

In this paper, the ions are treated as rigid bodies, and their densities are assumed to be low enough that ion-ion interactions can be ignored. Because the ions drift into regions of fresh bath gas, it is also assumed that the ions always encounter bath gas particles that are at equilibrium at the bath gas temperature.

The rotationally averaged velocity distribution for the ions at equilibrium (that is with no electric field present) is simply the Maxwellian distribution, namely

$$f_{\mathrm{T}}(\mathbf{v}) = \left(\frac{m}{2\pi k_B T^t}\right)^{3/2} \exp\left(-\frac{mv^2}{2k_B T^t}\right), \tag{1}$$

in which m is the mass of the ion, k_B is Boltzmann's constant, and T^t is the (translational) temperature of the ions. Because the ions are at equilibrium and the kinetic energy part of the Hamiltonian has a quadratic form, equipartition of energy occurs, so that

$$m\langle v_x^2\rangle = m\langle v_y^2\rangle = m\langle v_z^2\rangle = k_B T^t. \tag{2}$$

These relations define the ion temperature, which at equilibrium is an isotropic property and is equal to the bath gas temperature.

When an electric field is applied, the ion motions eventually reach a steady state and the ions adopt a fixed drift velocity. The distribution function describing this nonequilibrium situation becomes axially symmetric, and clearly cannot be represented by the isotropic form of Eq. (1). However, because the equilibrium distribution of Eq. (1) depends upon the square of the velocity, it naturally separates into components that are parallel and perpendicular to the field direction. As a first approximation, a nonequilibrium distribution function can be formed by simply treating these two components independently, that is [9,10]

$$f_{\mathrm{T}}(v_\perp, v_\parallel) = \left(\frac{m}{2\pi k_B T_\perp^t}\right)\left(\frac{m}{2\pi k_B T_\parallel^t}\right)^{1/2} \times \exp\left(-\frac{mv_\perp^2}{2k_B T_\perp^t} - \frac{m(v_\parallel - v_D)^2}{2k_B T_\parallel^t}\right), \tag{3}$$

in which $v_D=\langle v_z\rangle$ is the drift velocity of the ions, $v_\perp = \sqrt{v_x^2+v_y^2}$ and $v_\parallel = v_z$ are the velocity components perpendicular and parallel with the field direction, respectively, and $T_\perp^t$ and $T_\parallel^t$ are the corresponding temperatures associated with those directions, that is

$$k_B T_\perp^t = \frac{m}{2}\langle v_\perp^2\rangle, \tag{4}$$

$$k_B T_\parallel^t = m\langle (v_\parallel - v_D)^2\rangle. \tag{5}$$

The perpendicular and parallel temperatures simply reflect the anisotropy in the energy distribution due to the nonequilibrium state of the system, and their difference is a measure of this. By generalizing the temperature concept in this manner, it is possible to use equilibrium distribution functions as templates for approximating nonequilibrium ones.

The situation is similar for the velocity-averaged rotational distribution function of linear ions, which in the equilibrium case is given by

$$f_{\mathrm{R}}(\mathbf{J}) = \left(\frac{1}{2\pi I k_B T^r}\right)\exp\left(-\frac{J^2}{2Ik_BT^r}\right), \tag{6}$$

in which I is the moment of inertia of the ion, and $\mathbf{J}$ is its angular momentum (J_x, J_y, and J_z will be used to denote the components of the angular momentum expressed in the SF frame). At equilibrium, equipartition of energy occurs, so that the rotational temperature T^r is the same as the translational temperature T^t, and is isotropic. As with Eq. (1), the distribution function depends upon the square of the angular momentum, so that in the nonequilibrium situation, it can be generalized, with the introduction of directionally dependent temperatures, such as [11–14]

$$f_{\mathrm{R}}(J_\perp, J_\parallel) = \mathcal{N}\exp\left(-\frac{J_\perp^2}{2Ik_BT_\perp^{adf}} - \frac{J_\parallel^2}{2Ik_BT_\parallel^{adf}}\right), \tag{7}$$

in which $J_\perp = \sqrt{J_x^2 + J_y^2}$ and $J_\parallel = J_z$ are the SF components of the rotational angular momentum perpendicular and parallel to the field direction, respectively. The temperatures $T_\perp^{adf}$ and $T_\parallel^{adf}$ are distinct from but related to the SF frame rotational temperatures perpendicular and parallel to the field, $T_\perp^r$ and $T_\parallel^r$, defined by

$$k_BT_\perp^r = \frac{3}{2}\frac{\langle J_\perp^2\rangle}{2I}, \tag{8}$$

$$k_BT_\parallel^r = 3\frac{\langle J_\parallel^2\rangle}{2I}. \tag{9}$$

The factors of 3 arise from the fact that for a linear ion at equilibrium $\langle J^2\rangle/2I = k_BT$ since only two degrees of freedom are present. We have found that the distribution function of Eq. (7) is quite a good approximation to the nonequilibrium one, even for high field strengths. Details of its derivation and utility can be found in Refs. [11,13].

One would like to apply this philosophy of generalizing equilibrium distribution functions to the nonequilibrium case for general rigid bodies. It is for this case that an immediate problem arises, since the equilibrium rotational distribution function for a general rigid body is

$$f_{\mathrm{R}} = \left(\frac{1}{2\pi k_BT}\right)^{3/2}\left(\frac{1}{I_xI_yI_z}\right)^{1/2}\exp\left(-\frac{H}{k_BT}\right) \tag{10}$$

in which the classical rotational Hamiltonian, H, is given by

$$H = \tfrac{1}{2}\boldsymbol{\omega}\cdot\mathbf{I}\cdot\boldsymbol{\omega} = \tfrac{1}{2}\mathbf{J}\cdot\mathbf{I}^{-1}\cdot\mathbf{J}, \tag{11}$$

with $\boldsymbol{\omega}$ the angular velocity vector, $\mathbf{I}$ the moment of inertia tensor, and $\mathbf{I}^{-1}$ its inverse. In the SF frame, $\mathbf{I}$ is a second-rank tensor whose components depend upon the orientation of the body relative to the SF axes. Unfortunately, in the SF frame, this distribution function does not naturally separate into components along the Cartesian directions, so that in a nonequilibrium situation when the behavior in the z direction distinguishes itself from the x and y directions, this function will not be easily generalized, since it mixes all Cartesian components.

If $\mathbf{n}$ is the unit vector in the direction of $\boldsymbol{\omega}$ so that $\boldsymbol{\omega} = \omega\mathbf{n}$ then the distribution function becomes

$$f_{\mathrm{R}} = \mathcal{N}\exp\left(-\frac{I\omega^2}{2k_BT}\right), \tag{12}$$

in which $I = \mathbf{n}\cdot\mathbf{I}\cdot\mathbf{n}$ is the moment of inertia about the axis of rotation $\mathbf{n}$. This function does have a quadratic form in the angular velocity but only when referenced to the direction $\mathbf{n}$ rather than the SF frame. This direction changes as the body moves, and in particular changes with respect to the symmetry axis of the system.

One would like the express Eq. (10) in a form that naturally separates into Cartesian coordinates of the SF frame, in order to guide generalizations of the distribution function for the nonequilibrium situation. Section II introduces a vector quantity $\boldsymbol{\rho}$ that accomplishes this task. Its relation to other classical quantities and the equations of motion is discussed in Sec. III while Sec. IV demonstrates its utility for a particular system. The paper ends with summary conclusions in Sec. V.

II. THE $\boldsymbol{\rho}$ VECTOR

Let the body-fixed (BF) frame reside within the rigid body with its origin at the center of mass of the body, and its axes along the principal axes. In this frame, the moment of inertia tensor is diagonal, and for general ions, all three principal moments of inertia I_x, I_y, and I_z are distinct and nonzero. Let $\mathbf{A}$ be the matrix that transforms quantities between the SF and BF frames, so that if $\mathbf{L}$ is a vector of components of the angular momentum expressed in the BF frame, they are related to the components in the SF frame by $\mathbf{L} = \mathbf{AJ}$. It should be noted that in this context the SF frame has its origin at the center of mass of the rigid body but its axes are fixed in space along the lab coordinates. The Euler angles [15] will be employed, $\boldsymbol{\Omega} = \{\phi, \theta, \psi\}$ so that

$$\mathbf{A} = \begin{pmatrix} \cos\psi\cos\phi - \cos\theta\sin\phi\sin\psi & \cos\psi\sin\phi + \cos\theta\cos\phi\sin\psi & \sin\psi\sin\theta \\ -\sin\psi\cos\phi - \cos\theta\sin\phi\cos\psi & -\sin\psi\sin\phi + \cos\theta\cos\phi\cos\psi & \cos\psi\sin\theta \\ \sin\theta\sin\phi & -\sin\theta\cos\phi & \cos\theta \end{pmatrix} \tag{13}$$

In the BF frame, the distribution function of Eq. (10) becomes

$$f_{\mathrm{R}}(\mathbf{L}) = \left(\frac{1}{2\pi k_B T}\right)^{3/2}\left(\frac{1}{I_x I_y I_z}\right)^{1/2} \times \exp\left[-\frac{1}{2k_B T}\left(\frac{L_x^2}{I_x}+\frac{L_y^2}{I_y}+\frac{L_z^2}{I_z}\right)\right], \tag{14}$$

since $\mathbf{L}=\mathbf{I}\cdot\boldsymbol{\omega}$. Note that the normalization constant in Eq. (14) was chosen so that

$$1 = \int f_{\mathrm{R}}(\mathbf{L}) d\mathbf{L}. \tag{15}$$

Define the vector $\boldsymbol{\rho}$ whose components in the BF frame are given by

$$\rho_x^{\mathrm{BF}} = \frac{L_x}{\sqrt{I_x}}, \quad \rho_y^{\mathrm{BF}} = \frac{L_y}{\sqrt{I_y}}, \quad \rho_z^{\mathrm{BF}} = \frac{L_z}{\sqrt{I_z}}, \tag{16}$$

so that in matrix notation

$$\boldsymbol{\rho}^{\mathrm{BF}} = \mathbf{I}^{-1/2}\mathbf{L} = \mathbf{I}^{1/2}\boldsymbol{\omega}. \tag{17}$$

In terms of $\boldsymbol{\rho}^{\mathrm{BF}}$, the distribution function of Eq. (14) becomes

$$f_{\mathrm{R}}(\boldsymbol{\rho}) = \left(\frac{1}{2\pi k_B T}\right)^{3/2} \exp\left[-\frac{1}{2k_B T}(\rho_x^{\mathrm{BF}^2}+\rho_y^{\mathrm{BF}^2}+\rho_z^{\mathrm{BF}^2})\right] = \left(\frac{1}{2\pi k_B T}\right)^{3/2} \exp\left[-\frac{\rho^{\mathrm{BF}^2}}{2k_B T}\right], \tag{18}$$

with the normalization constant chosen so that

$$1 = \int f_{\mathrm{R}}(\boldsymbol{\rho}) d\boldsymbol{\rho}. \tag{19}$$

The distribution function of Eq. (18) is now expressed in terms of a purely quadratic function that treats equally all components in the BF frame. More importantly though, it maintains this form when transformed to the SF frame because this transformation is orthogonal, and preserves the magnitude of all vectors. In other words, if the components in the SF frame are denoted $\boldsymbol{\rho}^{\mathrm{SF}}$ then $\boldsymbol{\rho}^{\mathrm{SF}}=\mathbf{A}^T\boldsymbol{\rho}^{\mathrm{BF}}$ and since $\mathbf{A}^T\mathbf{A}=\mathbf{A}\mathbf{A}^T=\mathbf{1}$, it follows that $\rho^{\mathrm{SF}^2}=\rho^{\mathrm{BF}^2}$ so that the distribution function expressed in the SF frame is simply Eq. (18) with $\boldsymbol{\rho}^{\mathrm{BF}}$ replaced by $\boldsymbol{\rho}^{\mathrm{SF}}$. In other words, the form of the distribution function is invariant to the frame of reference.

From this point forward, in order to simplify the notation, the superscripts BF and SF will be dropped. Only the distinction in notation for the angular momentum vector will be retained. Thus, in either frame of reference it follows that at equilibrium

$$\langle \rho_x^2 \rangle = \langle \rho_y^2 \rangle = \langle \rho_z^2 \rangle = k_B T. \tag{20}$$

In the SF frame, a generalization of the rotational distribution function for general ions to the nonequilibrium case could take the form

$$f_{\mathrm{R}}(\rho_\perp, \rho_\parallel) = \left(\frac{1}{2\pi k_B T_\perp^r}\right)\left(\frac{1}{2\pi k_B T_\parallel^r}\right)^{1/2} \exp\left(-\frac{\rho_\perp^2}{2k_B T_\perp^r} - \frac{\rho_\parallel^2}{2k_B T_\parallel^r}\right), \tag{21}$$

in which $\rho_\perp = \sqrt{\rho_x^2+\rho_y^2}$, $\rho_\parallel = \rho_z$, and the rotational temperatures in the directions perpendicular and parallel to the field are given by

$$k_B T_\perp^r = \tfrac{1}{2}\langle \rho_\perp^2 \rangle, \tag{22}$$

$$k_B T_\parallel^r = \langle \rho_\parallel^2 \rangle. \tag{23}$$

Equation (21) now has a form that is analogous to Eqs. (3) and (7), and suggests that the best description of the nonequilibrium situation will be with $\boldsymbol{\rho}$ rather than with the angular momentum or angular velocity vectors.

Consider for a moment the case of linear rigid bodies. In this case, one of the principal moments of inertia is zero, and the remaining two are equal to a constant, I. In the BF frame, Eq. (16) shows that $\boldsymbol{\rho}=\mathbf{L}/\sqrt{I}$ so that in the SF frame, $\boldsymbol{\rho}=\mathbf{J}/\sqrt{I}$. In other words, $\rho_\parallel = J_\parallel/\sqrt{I}$ and $\rho_\perp = J_\perp/\sqrt{I}$, so that the distribution functions in ρ given by Eqs. (18) and (21) reduce to the forms already given by Eqs. (6) and (7), respectively. Note that with linear ions, the normalization must be done carefully since only two components of $\mathbf{J}$ (or $\boldsymbol{\rho}$) are linearly independent. This affects details of the normalization constant, and the form of the temperatures appearing in the distribution function. Details of this can be found in Refs. [11,13]. The main point though is that a general formulation in terms of $\boldsymbol{\rho}$ reduces in the linear case to the correct forms that have already been developed, so that the linear case is a subset of the more general formulation.

A similar reduction occurs for totally symmetric bodies for which all moments of inertia are equal to the same constant. In this case, as with the linear one, $\boldsymbol{\rho}=\mathbf{J}/\sqrt{I}$ and the $\boldsymbol{\rho}$ formalism reduces to a scaled angular momentum one.

In closing this section, consider the manner in which the $\boldsymbol{\rho}$ vector is described in terms of angular quantities. The distribution function for a general rigid body [Eq. (10)] depends explicitly upon the angles that determine the orientation of the body in the SF frame. This orientation determines the instantaneous value of the moment of inertia tensor, which is intimately coupled with the angular momentum (or angular velocity) in the exponent of the distribution function. For linear bodies, this angular dependence decouples from the angular momentum dependence, and the rotational kinetic energy depends only on the total angular momentum. Hence the angular dependence would appear only as a multiplicative constant in the distribution function, and disappears upon normalization. However, this is not true in the general case.

Let $f_{\mathrm{R}}(\mathbf{J},\boldsymbol{\Omega})$ represent the distribution function of Eq. (10) where now the explicit variable dependencies are shown. In practice, one usually is interested only in the distribution function that is averaged over $\boldsymbol{\Omega}$ but retains the dependence on $\mathbf{J}$. Because of the complex coupling between $\mathbf{J}$ and $\boldsymbol{\Omega}$, it is difficult to find the angular average of $f_{\mathrm{R}}(\mathbf{J},\boldsymbol{\Omega})$. In the SF frame, $\boldsymbol{\rho}=\mathbf{I}^{-1/2}\cdot\mathbf{J}$ so that each component of $\boldsymbol{\rho}$ is a combination of both angular momentum compo-

nents and angular dependencies through $\mathbf{I}$. Thus, following paths of constant $\boldsymbol{\rho}$ corresponds to following complicated combinations of both angular and angular momentum components, in such a manner as to keep the components of $\boldsymbol{\rho}$ constant. Using the relationship between $\mathbf{J}$ and $\boldsymbol{\rho}$ gives the Jacobian for the transformation from $(\mathbf{J},\boldsymbol{\Omega})$ to $(\boldsymbol{\rho},\boldsymbol{\Omega})$ as $|\mathbf{I}^{1/2}|$, so that $d\mathbf{J}=\sqrt{I_xI_yI_z}d\boldsymbol{\rho}$. The result of this transformation is that the integrals over angular coordinates are decoupled from the distribution, and reduce to unity after normalization. This decoupling is the strength of the $\boldsymbol{\rho}$ formalism.

III. BEHAVIOR OF $\boldsymbol{\rho}$

This section will consider the equations of motion for $\boldsymbol{\rho}$, as well as its relation to more commonly known descriptions of rigid body motion. In the BF frame, it is straightforward to transform the standard Euler equations of motion to give the equations of motion for $\boldsymbol{\rho}$, namely [15]

$$\sqrt{I_x}\dot{\rho}_x-\rho_y\rho_z\left(\sqrt{\frac{I_y}{I_z}}-\sqrt{\frac{I_z}{I_y}}\right)=\tau_x,$$

$$\sqrt{I_y}\dot{\rho}_y-\rho_z\rho_x\left(\sqrt{\frac{I_z}{I_x}}-\sqrt{\frac{I_x}{I_z}}\right)=\tau_y,$$

$$\sqrt{I_z}\dot{\rho}_z-\rho_x\rho_y\left(\sqrt{\frac{I_x}{I_y}}-\sqrt{\frac{I_y}{I_x}}\right)=\tau_z, \tag{24}$$

in which τ_x, τ_y, and τ_z are the components of the torque on the body, expressed in BF frame coordinates. For linear ions (when $I_x=I_y=I$ and $I_z=\omega_z=0$) or spherical ions (when $I_x=I_y=I_z=I$), the angular velocity, angular momentum, and $\boldsymbol{\rho}$ vectors are all parallel, and differ only by a scaling of I, so that the equations of motion predict the same motions. However, for a general rigid body, the motion of $\boldsymbol{\rho}$ is distinct from that of either the angular velocity or the angular momentum.

Consider the motion of a body when all external torques are zero. In this case, the energy of the system, H, is conserved, as is the total angular momentum $\mathbf{J}$ in the SF frame. In the BF frame, imagining that the axes measure the components of $\boldsymbol{\rho}$, these conserved quantities are expressed as

$$2H=\rho_x^2+\rho_y^2+\rho_z^2, \tag{25}$$

$$J^2=L^2=I_x\rho_x^2+I_y\rho_y^2+I_z\rho_z^2. \tag{26}$$

The first equation defines a sphere of radius $\sqrt{2H}$, while the second describes an ellipsoid with semimajor axes $L/\sqrt{I_x}$, $L\sqrt{I_y}$, and $L/\sqrt{I_z}$. The intersection of these two surfaces gives the paths along which the motion of $\boldsymbol{\rho}$ is constrained. This geometrical interpretation is completely analogous to the usual construction of the Binet ellipsoid [15], except that in the latter case the BF frame angular momentum is used as a reference rather than $\boldsymbol{\rho}$. In this regard, the description of the motion in the BF frame can be equally well described by $\boldsymbol{\rho}$, as with other standard approaches.

In the SF frame, the situation differs. The Poinsot construction is the usual means to analyze geometrically the motion of torque-free rigid bodies [15]. This relies upon certain relationships between the angular velocity and angular momentum vectors. These same relationships do not exist for $\boldsymbol{\rho}$. For example, it can be shown that in the SF frame that $\boldsymbol{\rho}\cdot\mathbf{J}$ and $\boldsymbol{\rho}\cdot\boldsymbol{\omega}$ both vary in time, even when $\mathbf{J}$ is fixed. Thus, in the general case, the motion of $\boldsymbol{\rho}$ does not maintain any fixed relationship with either the angular velocity or angular momentum.

What can be said with certainty is that the components of $\boldsymbol{\rho}$ in the SF frame, for a torque-free body, lie on a sphere of radius $\sqrt{2H}$, precisely as in the BF frame. Since $\boldsymbol{\rho}=\mathbf{I}^{-1/2}\cdot\mathbf{J}$, when $\mathbf{J}$ is constant, $\dot{\boldsymbol{\rho}}=\dot{\mathbf{I}}^{-1/2}\cdot\mathbf{J}$. Even when $\mathbf{J}$ is constant, $\boldsymbol{\rho}$ changes with time. The change in $\boldsymbol{\rho}$ is linked solely with the change in the moment of inertia tensor as the body moves in space. More specifically, the changes that are along the angular momentum vector are the ones that will contribute to changing the direction of $\boldsymbol{\rho}$. Unfortunately, there is no simple way to gauge the magnitude of these changes, and even a qualitative description of them is difficult in the general case.

Finally, a few words should be said concerning the relationship between $\boldsymbol{\rho}$ and the usual action-angle coordinates used to describe rigid body motion. If p_ϕ, p_θ, and p_ψ denote the momenta conjugate to ϕ, θ, and ψ, and $\mathbf{p}$ is a vector of these momentum components, then $\mathbf{p}$ is related to $\mathbf{J}$ by

$$\mathbf{p}=\mathbf{C}\mathbf{J}, \tag{27}$$

in which

$$\mathbf{C}=\begin{pmatrix}0 & 0 & 1\\ \cos\phi & \sin\phi & 0\\ \sin\theta\sin\phi & -\sin\theta\cos\phi & \cos\theta\end{pmatrix}. \tag{28}$$

The z components of the angular momentum in the SF and BF frames are equal to p_ϕ and p_ψ, respectively. The relation of Eq. (27) can be inverted, so that from a SF frame perspective the rotational Hamiltonian can be written as

$$2H=\mathbf{J}\cdot\mathbf{I}_{\mathrm{SF}}^{-1}\cdot\mathbf{J}=\mathbf{J}^T\mathbf{A}^T\mathbf{I}_{\mathrm{BF}}^{-1}\mathbf{A}\mathbf{J}=\mathbf{p}^T\mathbf{D}^T\mathbf{I}_{\mathrm{BF}}^{-1}\mathbf{D}\mathbf{p}, \tag{29}$$

in which $\mathbf{I}_{\mathrm{BF}}$ is the diagonal moment of inertia tensor in the BF frame, and

$$\mathbf{D}=\mathbf{A}\mathbf{C}^{-1}=\frac{1}{\sin\theta}\begin{pmatrix}\sin\psi & \sin\theta\cos\psi & -\cos\theta\sin\psi\\ \cos\psi & -\sin\theta\sin\psi & -\cos\theta\cos\psi\\ 0 & 0 & \sin\theta\end{pmatrix}. \tag{30}$$

Substituting the expression for $\mathbf{D}$ into Eq. (29) then allows one to express H in terms of a proper set of conjugate variables, from which equations of motion could be obtained using Hamilton's equations. Using Eq. (27) also gives a relation between $\mathbf{p}$ and $\boldsymbol{\rho}$, namely

$$\boldsymbol{\rho}=\mathbf{I}_{\mathrm{SF}}^{-1/2}\mathbf{J}=\mathbf{A}^T\mathbf{I}_{\mathrm{BF}}^{-1/2}\mathbf{A}\mathbf{C}^{-1}\mathbf{p}=\mathbf{A}^T\mathbf{I}_{\mathrm{BF}}^{-1/2}\mathbf{D}\mathbf{p}. \tag{31}$$

Equation (31) relates the components of $\boldsymbol{\rho}$ in the SF frame to the momenta conjugate to $\boldsymbol{\Omega}$. Inverting this equation then relates these momenta to $\boldsymbol{\rho}$, and one might be tempted to find a generating function of the F_2 type [15] to transform from the $(\boldsymbol{\Omega},\mathbf{p})$ conjugate set to a new one involving $\boldsymbol{\rho}$ and a, as yet undetermined, set of conjugate coordinates. However, it is easy to show that such a generating function does not

exist, implying that the relation of Eq. (31) is not a canonical transformation. That is, there is no set of coordinates conjugate to $\boldsymbol{\rho}$.

This must be the case because it is well known that using components of the angular momentum in the BF frame, H can be written [17,18]

$$2H = \frac{1}{I_y}L^2 - \frac{1}{2}\left(\frac{1}{I_x} - \frac{1}{I_z}\right)\eta^2, \tag{32}$$

in which

$$\eta^2 = (1+\kappa)L_z^2 - (1-\kappa)L_x^2, \tag{33}$$

with

$$\kappa = \frac{\dfrac{2I_xI_z}{I_y} - I_z - I_x}{I_z - I_x}. \tag{34}$$

The set (L, η) of momentum variables are proper action variables with corresponding conjugate angles, and the equations of motion derived from Eq. (32) using Hamilton's equations will depend upon them. One cannot specify the Hamiltonian with fewer than these two action variables. In the $\boldsymbol{\rho}$ formalism, $2H=\rho^2$ so that the Hamiltonian depends upon only one variable. This therefore cannot be a proper action variable. In other words, one cannot obtain equations of motion by employing Hamilton's equations using the Hamiltonian expressed in terms of $\boldsymbol{\rho}$. Rather one must resort to one of the usual formulations either in terms of angular frequencies or action-angle variables. The BF frame description still remains as one of the best ways for solving the equations of motion, and in practice we calculate the angular frequency components using Eq. (24), and then calculate the BF and SF frame components of $\boldsymbol{\rho}$ for analysis purposes.

The net result of this extended discussion is to show that $\boldsymbol{\rho}$ is not a new dynamical variable, in the sense of serving as part of an action-angle variable pair. While the BF or SF components of $\boldsymbol{\rho}$ can be related to well established descriptions of rotational motions, the real utility of the formalism is in simplifying the form of the general rotational Hamiltonian, thereby leading to a simple form for the equilibrium distribution function. This was the purpose in constructing the $\boldsymbol{\rho}$ formalism, and in this regard, it leads to simplifications that are not possible with any of the other variables used to describe general, rigid body motion.

IV. DISCUSSION

In order to test the utility of the $\boldsymbol{\rho}$ formalism, distribution functions will be examined from ion mobility simulations. In particular, the drifting of H_2O^+ in a bath of helium atoms will be used as an example. The details of this simulation are given elsewhere [16,19]. For the present purpose, it suffices to say that the system is described classically using a molecular dynamics algorithm that correctly accounts for the energy exchange of the ion with the bath gas. In all cases, the bath gas is maintained at a constant temperature of 300 K and a constant number density of 0.1 particles/nm^3. Two scenarios will be considered: ion motion with no external field present (the equilibrium case), and ions drifting with an external electric field of 30 Td [the townsend unit (Td) expresses the electric field strength relative to the bath gas number density]. This field strength is sufficient to significantly perturb the system from equilibrium, so it will provide a good example of a nonequilibrium scenario. While these two cases are clearly not exhaustive, they will demonstrate quite effectively the utility of the $\boldsymbol{\rho}$ formalism. Note that the ion is treated as a rigid body in the simulations, and that all three of its principal moments of inertia differ from each other.

Note that this case is not the most general since the bath gas is atomic. For a molecular ion in an atomic bath, the total rotational and translational temperatures are the same [20]. However, this equality does not generally hold if the bath gas is molecular, with rotational and vibrational degrees of freedom. Even in the more general situation though, the $\boldsymbol{\rho}$ formalism should apply equally well.

Table I reports the values of a number of averaged quantities for the equilibrium and nonequilibrium cases both measured within the BF and SF frames. In all cases, the averages of the components of either the angular momentum or $\boldsymbol{\rho}$ are zero. In the ion mobility system there is no mechanism to induce a preferred direction for the angular momentum, that is in an ensemble of ions equal numbers are spinning clockwise as anticlockwise. This causes the ensemble average of the components of the angular momentum to be zero. This same argument applies to the components of $\boldsymbol{\rho}$, and demonstrates that while $\boldsymbol{\rho}$ is not precisely the same as either the angular velocity or the angular momentum, it still retains the characteristics of these angular quantities.

Consider first the equilibrium case when no external field is present. In this case, the rotational temperature should be the same as the bath gas temperature (300 K), and this value should be isotropic. In the BF frame, the angular momentum can be used to calculate this temperature since

$$\frac{\langle L_x^2\rangle}{I_x} = \frac{\langle L_y^2\rangle}{I_y} = \frac{\langle L_z^2\rangle}{I_z} = k_BT^r, \tag{35}$$

and the results of Table I show that the predicted temperature is essentially identical to the bath gas one, and that the prediction of this temperature using the different components each yield the same value. Note that the averages of the squares of the components of $\mathbf{L}$ are not equal because the principal moments of inertia in each direction differ. However, equipartition of energy has occurred, as demonstrated by the calculated temperatures. This also shows that the molecular dynamics code correctly predicts the expected behavior.

Alternatively, using the components of $\boldsymbol{\rho}$ one has

$$\langle \rho_x^2\rangle = \langle \rho_y^2\rangle = \langle \rho_z^2\rangle = k_BT^r, \tag{36}$$

which by construction in the BF frame leads to temperature predictions that are identical to those obtained from averages of $\mathbf{L}$. Notice though that because the components of $\boldsymbol{\rho}$ already incorporate the principal moments of inertia, each component is on an equal footing so that the averages of the

TABLE I. Values of calculated ensemble averages for H_2O^+—He at 300 K with no external field present (labeled "Equilibrium") and with an external field of 30 Td (labelled "Nonequilibrium"). Bracketed numbers indicate the estimated error in the last digit of the reported values. Note that for these calculations, the principal moments of inertia of the ion, in units of amu nm^2, were $I_x = 1.933\,12 \times 10^{-2}$, $I_y = 5.929\,35 \times 10^{-3}$, and $I_z = 1.340\,18 \times 10^{-2}$, so that $I_{\text{eff}} = 1.288\,74 \times 10^{-2}$ and $I' = 1.190\,54 \times 10^{-2}$.

Parameter	Equilibrium	Nonequilibrium
Body-fixed frame values		
$\langle L_x \rangle$ (amu nm^2/ps)	0.000(1)	0.000(1)
$\langle L_y \rangle$ (amu nm^2/ps)	0.000(1)	0.000(1)
$\langle L_z \rangle$ (amu nm^2/ps)	0.000(1)	0.000(1)
$\langle L_x^2 \rangle$ [(amu nm^2/ps)^2]	0.04836(8)	0.127(1)
$\langle L_y^2 \rangle$ [(amu nm^2/ps)^2]	0.01483(2)	0.0385(1)
$\langle L_z^2 \rangle$ [(amu nm^2/ps)^2]	0.03357(4)	0.0877(1)
$\langle L_x^2 \rangle / I_x k_B$ (K)	300.9(5)	790(5)
$\langle L_y^2 \rangle / I_y k_B$ (K)	300.8(4)	780(5)
$\langle L_z^2 \rangle / I_z k_B$ (K)	301.3(4)	787(3)
$\langle \boldsymbol{\rho}_x \rangle$ (amu$^{1/2}$ nm/ps)	0.000(1)	0.000(1)
$\langle \boldsymbol{\rho}_y \rangle$ (amu$^{1/2}$ nm/ps)	0.000(1)	0.000(1)
$\langle \boldsymbol{\rho}_z \rangle$ (amu$^{1/2}$ nm/ps)	0.000(1)	0.000(1)
$\langle \boldsymbol{\rho}_x^2 \rangle$ [amu(nm/ps)^2]	2.502(4)	6.57(4)
$\langle \boldsymbol{\rho}_y^2 \rangle$ [amu(nm/ps)^2]	2.501(3)	6.48(4)
$\langle \boldsymbol{\rho}_z^2 \rangle$ [amu(nm/ps)^2]	2.505(3)	6.54(3)
$\langle \boldsymbol{\rho}_x^2 \rangle / k_B$ (K)	300.9(5)	790(5)
$\langle \boldsymbol{\rho}_y^2 \rangle / k_B$ (K)	300.8(4)	780(5)
$\langle \boldsymbol{\rho}_z^2 \rangle / k_B$ (K)	301.3(4)	787(3)
Space-fixed frame values		
$\langle J_x \rangle$ (amu nm^2/ps)	0.000(1)	0.000(1)
$\langle J_y \rangle$ (amu nm^2/ps)	0.000(1)	0.000(1)
$\langle J_z \rangle$ (amu nm^2/ps)	0.000(1)	0.000(1)
$\langle J_x^2 \rangle$ [(amu nm^2/ps)^2]	0.03225(3)	0.0862(1)
$\langle J_y^2 \rangle$ [(amu nm^2/ps)^2]	0.03227(5)	0.0862(2)
$\langle J_z^2 \rangle$ [(amu nm^2/ps)^2]	0.03224(6)	0.0807(2)
$\langle J_x^2 \rangle / I_{\text{eff}} k_B$ (K)	301.0(3)	804(1)
$\langle J_y^2 \rangle / I_{\text{eff}} k_B$ (K)	301.2(6)	804(2)
$\langle J_z^2 \rangle / I_{\text{eff}} k_B$ (K)	300.9(6)	753(2)
$\langle \boldsymbol{\rho}_x \rangle$ (amu$^{1/2}$ nm/ps)	0.000(1)	0.000(1)
$\langle \boldsymbol{\rho}_y \rangle$ (amu$^{1/2}$ nm/ps)	0.000(1)	0.000(1)
$\langle \boldsymbol{\rho}_z \rangle$ (amu$^{1/2}$ nm/ps)	0.000(1)	0.000(1)
$\langle \boldsymbol{\rho}_x^2 \rangle$ [amu(nm/ps)^2]	2.502(3)	6.66(1)
$\langle \boldsymbol{\rho}_y^2 \rangle$ [amu(nm/ps)^2]	2.504(4)	6.65(1)
$\langle \boldsymbol{\rho}_z^2 \rangle$ [amu(nm/ps)^2]	2.502(4)	6.28(1)
$\langle \boldsymbol{\rho}_x^2 \rangle / k_B$ (K)	300.9(4)	801(1)
$\langle \boldsymbol{\rho}_y^2 \rangle / k_B$ (K)	301.2(6)	800(1)
$\langle \boldsymbol{\rho}_z^2 \rangle / k_B$ (K)	300.9(5)	755(1)

squares of the components of $\boldsymbol{\rho}$ are the same in all three Cartesian directions.

However, imagine one wanted to calculate these same quantities in the SF frame. This is straightforward using the SF components of $\boldsymbol{\rho}$ since Eq. (36) is valid in either frame so that the temperatures are calculated in precisely the same manner as in the BF frame. The entries in Table I show that these values agree with the correct overall temperature. How would the same quantities be calculated using the SF frame components of the angular momentum? Unambiguously, the total rotational energy must be related to the total rotational temperature according to $\langle H \rangle = 3k_B T^r/2$ but $\langle H \rangle$ is not easily decomposed into ensemble averages over angular momentum components directly.

Instead, consider Eq. (35) from which it must follow that (since the magnitude of the angular momentum is invariant with respect to the frame of reference)

$$\langle L^2 \rangle = \langle J^2 \rangle = 3I_{\text{eff}} k_B T^r, \tag{37}$$

with

$$I_{\text{eff}} = \tfrac{1}{3}(I_x + I_y + I_z), \tag{38}$$

from which the general relation follows

$$\frac{\langle J \rangle}{2I_{\text{eff}}} = \langle \mathbf{J} \cdot \mathbf{I}^{-1} \cdot \mathbf{J} \rangle. \tag{39}$$

In the SF frame, $\mathbf{J} = \mathbf{I}^{1/2} \cdot \boldsymbol{\rho}$ so that using the distribution function in terms of $\boldsymbol{\rho}$ allows the averages of the squares of the angular momentum components to be evaluated. After some straightforward but somewhat tedious algebra, one obtains

$$\langle J_x^2 \rangle = \tfrac{1}{5}(3I_{\text{eff}} + 2I')\langle \rho_x^2 \rangle + \tfrac{1}{5}(I_{\text{eff}} - I')\langle \rho_y^2 \rangle + \tfrac{1}{5}(I_{\text{eff}} - I')\langle \rho_z^2 \rangle, \tag{40}$$

$$\langle J_y^2 \rangle = \tfrac{1}{5}(I_{\text{eff}} - I')\langle \rho_x^2 \rangle + \tfrac{1}{5}(3I_{\text{eff}} + 2I')\langle \rho_y^2 \rangle + \tfrac{1}{5}(I_{\text{eff}} - I')\langle \rho_z^2 \rangle,$$

$$\langle J_z^2 \rangle = \tfrac{1}{5}(I_{\text{eff}} - I')\langle \rho_x^2 \rangle + \tfrac{1}{5}(I_{\text{eff}} - I')\langle \rho_y^2 \rangle + \tfrac{1}{5}(3I_{\text{eff}} + 2I')\langle \rho_z^2 \rangle,$$

in which

$$I' = \tfrac{1}{3}(\sqrt{I_x I_y} + \sqrt{I_y I_z} + \sqrt{I_x I_z}). \tag{41}$$

At equilibrium, Eq. (36) gives the averages of the SF frame components of $\boldsymbol{\rho}$ which along with Eqs. (40) gives

$$\langle J_x^2 \rangle = \langle J_y^2 \rangle = \langle J_z^2 \rangle = I_{\text{eff}} k_B T^r. \tag{42}$$

Equations (37) and (42) are completely consistent and show that I_{eff} is the proper moment of inertia to use when scaling the angular momentum averages in the SF frame to give rotational temperatures. The results of this scaling are shown in Table I, where it can be seen that in the equilibrium case, all the components predict a rotational temperature that is the same as the bath gas temperature, as it should be.

Some distribution functions are examined for the equilibrium case in the top panels of Figs. 1–3. The upper panel of Fig. 1 plots the equilibrium distribution functions in the BF frame as a function of the angular momentum components. The symbols give the values calculated from the molecular dynamics simulation while the solid lines plot the corre-

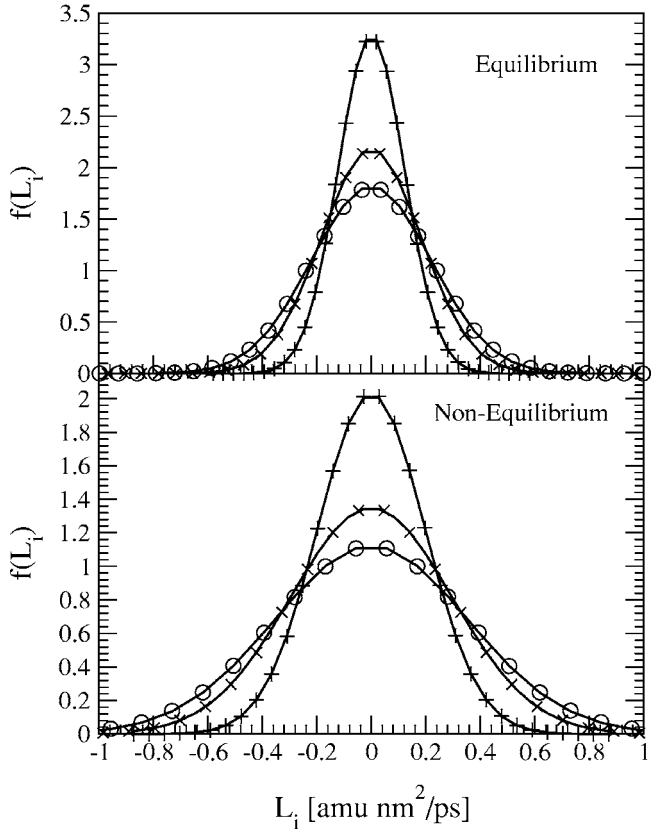

FIG. 1. Plots of the rotational distribution function as a function of angular momentum in the BF frame. In both panels, the circles, pluses, and crosses represent values for the $i=x$, y, and z components, respectively, obtained from molecular dynamics calculations. The corresponding solid lines are predictions of Eq. (43). The upper panel shows results for the equilibrium case when the system is equilibrated at 300 K. The lower panel shows results for the nonequilibrium case when the total rotational temperature is 786 K.

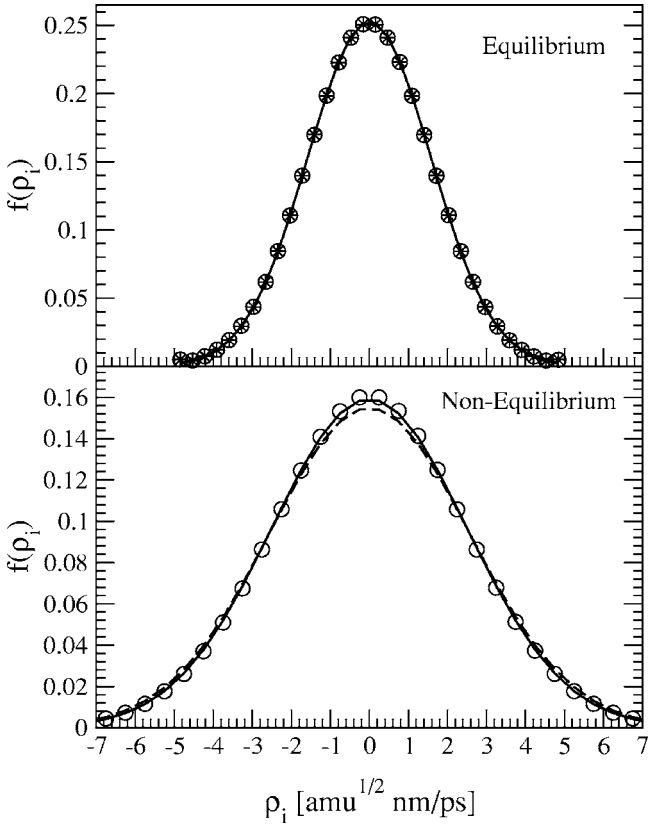

FIG. 2. Plots of the rotational distribution function as a function of the components of $\boldsymbol{\rho}$ in the SF frame. In the upper panel, the equilibrium case, the circles, pluses, and crosses represent values for the $i=x$, y, and z components, respectively, obtained from molecular dynamics calculations. The corresponding solid lines are predictions of Eq. (44) using a temperature of 300 K. In the lower panel, the nonequilibrium case, the circles represent molecular dynamics values for the z component while the dashed line gives the x and y component values. The solid line is the prediction of Eq. (44) using a temperature of 755 K for the z component.

sponding functions derived from integrating Eq. (14), namely

$$f_{\mathrm{R}}(L_i) = \left(\frac{1}{2\pi I_i k_B T}\right)^{1/2} \exp\left[-\frac{L_i^2}{2I_i k_B T}\right], \tag{43}$$

in which $i=x$, y, or z. The agreement is excellent. Identical agreement would have been obtained had the distribution functions been plotted as functions of the components of $\boldsymbol{\rho}$, except that the curves for each component would have been identical.

In the SF frame, the situation differs. In terms of $\boldsymbol{\rho}$, the distribution function nicely separates into Cartesian components, each of which has the same functional form, namely

$$f_{\mathrm{R}}(\rho_i) = \left(\frac{1}{2\pi k_B T^r}\right)^{1/2} \exp\left[-\frac{\rho_i^2}{2k_B T^r}\right], \tag{44}$$

in which $i=x$, y, or z. The calculated distributions and predictions of Eq. (44) for each component is shown in the upper panel of Fig. 2. All the components predict precisely the same function, and the agreement with the equilibrium function is excellent. Again, this simply verifies that the molecular dynamics code is functioning properly.

On the other hand, the distribution functions as a function of angular momentum are not so easy to quantify. Integrating analytically the distribution function of Eq. (10) over all the Euler angles is not easily done analytically. However, a different approach can be used, considering that both the first and second order moments [via Eq. (42)] are known precisely. One can construct an approximate form that will match these moments, that is

$$g_{\mathrm{R}}(\mathbf{J}) = \left(\frac{1}{2\pi I_{\mathrm{eff}} k_B T^r}\right)^{3/2} \exp\left[-\frac{\boldsymbol{J}^2}{2I_{\mathrm{eff}} k_B T^r}\right]. \tag{45}$$

This form has a number of attractive qualities. The form separates the contributions to the distribution along the Cartesian directions, so that one can easily associate perpendicular and parallel components. It also reduces to the known forms for the linear and fully symmetric ion cases. In the upper panel of Fig. 3, the z component of this distribution is compared with the simulation results. The agreement is reasonable but Eq. (45) underestimates the correct distribution

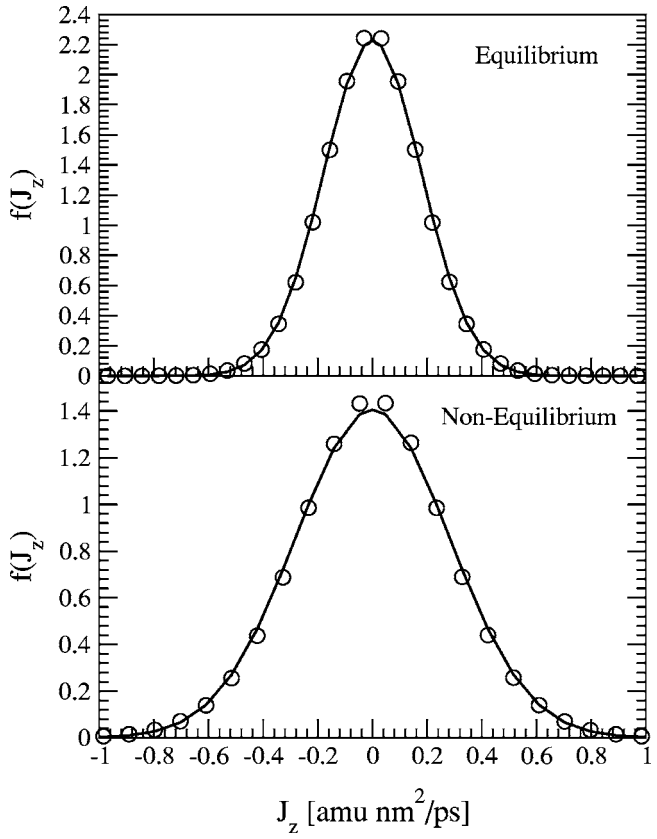

FIG. 3. Plots of the rotational distribution function as a function of the z component of the angular momentum in the SF frame. In the upper panel, the equilibrium case, the circles represent values obtained from molecular dynamics calculations. The solid line is a plot using Eq. (45) with a temperature of 300 K and a value $I_{\text{eff}} = 1.288\,74 \times 10^{-2}$ amu nm^2. In the lower panel, the nonequilibrium case, the circles represent molecular dynamics values. The solid line is the prediction of Eq. (45) using the I_{eff} above and a temperature of 753 K.

when J_z is near zero. The agreement is certainly not as good as that seen in the upper panel of Fig. 2.

One major drawback of Eq. (45) is that at best it is a good approximation but it can never match the correct distribution function. This can immediately be seen by considering the value for $J=0$. When $J=0$, Eq. (45) gives $g_{\text{R}} = 1/(2\pi I_{\text{eff}} k_B T^r)^{3/2}$. However, the correct distribution function of Eq. (10) gives in this limit $f_{\text{R}} = 1/(2\pi k_B T^r)^{3/2}/\sqrt{I_x I_y I_z}$. These two values are the same only if $I_{\text{eff}}^3 = I_x I_y I_z$. A short analysis shows that this equality cannot be satisfied for real and positive numbers I_x, I_y, and I_z unless $I_x = I_y = I_z$. Thus, in the general case, Eq. (45) cannot match the correct distribution precisely.

Consider now the nonequilibrium case. The electric field is applied along the SF frame z axis, and the averages in this frame, as seen in Table I, immediately develop cylindrical symmetry about this direction, with the z component averages differing from those in the x and y directions, which themselves are equal. In the BF frame, though, this distinction between the Cartesian directions does not exist. The collision environment in the drifting process ensures that equipartition of energy occurs within the BF frame even in the nonequilibrium case. This does not occur in the SF frame because as the ion drifts, the angular momentum becomes aligned perpendicular to the electric field, and this produces an anisotropy in the energy distribution in different Cartesian directions.

Returning to the BF frame results, although there is more fluctuation in the molecular dynamics results, the temperatures calculated from the averages of the components of $\mathbf{L}$ [as per Eq. (35)] or the values of the averages of the squares of the components of $\boldsymbol{\rho}$ show that equipartition occurs. The total rotational temperature is an average of the values for the three components, yielding a value of $T^r = 786$ K. This temperature is significantly higher than the bath gas temperature. The ion gains energy from the field, and this is eventually deposited, via collisions, into translational and rotational degrees of freedom, causing heating.

Although in a steady state, the drifting ion is far from thermal equilibrium, the distribution function in the BF frame is simply the equilibrium of Eq. (43) evaluated with the total rotational temperature T^r, as seen from the excellent agreement in the lower panel of Fig. 1.

Although this simple form exists in the BF frame, it is not easily transformed to the SF frame because of the nonuniform sampling of ion orientations. In the SF frame, the $\boldsymbol{\rho}$ formalism again produces reasonable results. It allows one to formulate rotational temperatures in the parallel and perpendicular field directions through averages of the components in the different Cartesian directions, that is applying Eq. (36) to the averages of each component of $\boldsymbol{\rho}$ gives $\langle \rho_x^2 \rangle = \langle \rho_y^2 \rangle = k_B T_\perp^r$ and $\langle \rho_z^2 \rangle = k_B T_\parallel^r$. The results in Table I show that the average rotational temperature perpendicular to the field is 800 K while that parallel to the field is 755 K. A similar extension can be made using the averages of the components of the angular momentum by generalizing Eq. (42) to the nonequilibrium case giving $\langle J_x^2 \rangle = \langle J_y^2 \rangle = I_{\text{eff}} k_B \tilde{T}_\perp^r$ and $\langle J_z^2 \rangle = I_{\text{eff}} k_B \tilde{T}_\parallel^r$. The results in Table I show that these rotational temperatures perpendicular and parallel to the field are 804 and 753 K, respectively.

These temperatures are similar but distinct from $T_\perp^r$ and $T_\parallel^r$. In fact, these can be related using Eqs. (40) to give

$$\tilde{T}_\perp^r = T_\perp^r + \frac{1}{5}\left(\frac{I' - I_{\text{eff}}}{I_{\text{eff}}}\right)(T_\perp^r - T_\parallel^r),$$

$$\tilde{T}_\parallel^r = T_\parallel^r - \frac{2}{5}\left(\frac{I' - I_{\text{eff}}}{I_{\text{eff}}}\right)(T_\perp^r - T_\parallel^r). \tag{46}$$

It can be seen that each temperature from one set is a mixture of both the perpendicular and parallel temperatures in the other set, and that this depends upon the difference between the moments of inertia I_{eff} and I'. Interestingly, these two distinct ways of specifying the perpendicular and parallel temperatures exist only for general bodies. For linear or fully symmetric bodies the two sets of temperatures are identical. However, it should be pointed out that even for general bodies, the total rotational temperature is the same regardless of the set one chooses, since it is straightforward to show that

$$T^r = \tfrac{1}{3}(2T^r_\perp + T_\parallel) = \tfrac{1}{3}(2\tilde{T}^r_\perp + \tilde{T}^r_\parallel). \quad (47)$$

Although both sets of temperatures are well defined, their utility in forming distribution functions differ. Using the temperatures associated with averages of $\boldsymbol{\rho}$ allows one to generalize the distribution function for the nonequilibrium case using the form of Eq. (21). The z component of this distribution is compared with simulation results in the lower panel of Fig. 2, where very good agreement can be seen. For comparison, the simulation derived distribution in the x and y directions is shown as a dashed line. There is clearly a difference between the distributions in these directions, and the results in either direction can be accurately described by Eq. (21) with the appropriately defined temperatures.

In contrast, the distributions as functions of the SF components of $\mathbf{J}$ have the same difficulty as encountered in the equilibrium case. If one wishes to use the rotational temperatures defined with the angular momentum components, then the distribution function of Eq. (45) can be employed as an approximation, since it will correctly reproduce these temperatures. Using this form, generalized with differing parallel and perpendicular temperatures in analogy with Eq. (3), allows predictions to be made once I_{eff} is calculated. This prediction for the z component is compared with simulation results in the lower panel of Fig. 3. As with the equilibrium case, the predicted curve underestimates the correct distribution function near $J_z=0$, giving agreement that is at best moderately good.

While the temperatures defined using the angular momentum components are well defined, and may be very relevant for experimental measurements, there is no well-defined procedure for using them to generalize the rotational distribution function. The temperatures defined using the components of $\boldsymbol{\rho}$ directly correlate with a well-defined distribution function generalized for nonequilibrium situations. However, they may not be as clearly connected with experimental measurement. The relation between the two sets, given by Eqs. (46), can be used to relate these. In practice, for mobility experiments, the difference between the perpendicular and parallel temperatures is typically 10–15% of the total, and given the relative closeness of the I' and I_{eff} values, it happens that the temperatures predicted using either the $\mathbf{J}$ or $\boldsymbol{\rho}$ formalisms are almost identical. This is seen in the data of Table I.

In closing, one caveat must be given concerning Eqs. (46). Strictly speaking, these relations are approximate because they were derived from Eqs. (40) which was obtained by integrating angular functions over a uniform distribution. In the nonequilibrium situation, the distribution function becomes a nonuniform function of $\boldsymbol{\Omega}$ so that the integrals performed analytically in obtaining Eqs. (40) then become approximate. While the relations used to define the rotational temperatures with either $\mathbf{J}$ or $\boldsymbol{\rho}$ still are valid, the relationship between the two sets, given by Eqs. (46), could break down if the angular part of the distribution function deviates substantially from uniformity.

V. CONCLUSIONS

A variety of experiments require the description of the motion of general rigid bodies from the perspective of a space-fixed frame. In many cases, the description of the rotational motion of such bodies is simple and straightforward in a body-fixed frame of reference. However, information in this frame (apart from the total rotational temperature or other averages that are invariant under the transformation from the body-fixed to the space-fixed frame) is difficult to transform to the space-fixed frame. While the angular momentum is a natural and appropriate variable for describing rotational motion, its components in the SF frame appear coupled with angular variables in the distribution function. For this reason, the vector $\boldsymbol{\rho}$ was defined so that $\boldsymbol{\rho}=\mathbf{I}^{-1/2}\cdot\mathbf{J}=\mathbf{I}^{1/2}\cdot\boldsymbol{\omega}$. The rotational Hamiltonian for a general rigid body adopts a simple quadratic form in both the body-fixed and space-fixed frames when expressed in terms of the components of $\boldsymbol{\rho}$, and this form naturally delineates contributions in the different Cartesian directions.

For this reason, it is particularly attractive for generalizing distribution functions for systems having cylindrical symmetry. It was demonstrated that when expressed in terms of the components of $\boldsymbol{\rho}$ the distribution function, even in a system far from equilibrium, can be approximated by simple functional forms. This is possible because the components of $\boldsymbol{\rho}$ are particularly well suited to this task. The same distributions expressed as functions of some other variable, such as the angular momentum, become complex and difficult to analyze and approximate analytically.

In special cases, such as for linear or spherically symmetric bodies, the $\boldsymbol{\rho}$ formalism simply reduces to a scaling of the angular momentum, in terms of which distributions are already well established. Thus, in all cases, the $\boldsymbol{\rho}$ formalism should be employed to describe rotational motions, since it performs correctly both for general bodies, and those with special symmetry.

ACKNOWLEDGMENTS

This work was supported by a grant from the Natural Sciences and Engineering Research Council of Canada, and the Canada Foundation for Innovation. Computing time on the WestGrid cluster at the University of British Columbia, Canada is also also gratefully acknowledged ⟨www.westgrid.ca⟩.

[1] E. A. Mason and E. W. McDaniel, *Transport Properties of Ions in Gases* (Wiley, New York, 1988).

[2] S. Harich and A. M. Wodtke, J. Chem. Phys. **107**, 5983 (1997).

[3] V. Aquilanti, D. Ascenzi, D. Cappelletti, R. Fedeli, and F. Pirani, J. Phys. Chem. A **101**, 7648 (1997).

[4] V. Aquilanti, D. Ascenzi, D. Cappelletti, M. de Castro, and F. Pirani, J. Chem. Phys. **109**, 3898 (1998).

[5] V. Aquilanti, D. Ascenzi, M. D. Vitores, F. Pirani, and D. Cappelletti, J. Chem. Phys. **111**, 2620 (1999).
[6] J. R. Fair and D. J. Nesbitt, J. Chem. Phys. **111**, 6821 (1999).
[7] T. Covey and D. J. Douglas, J. Am. Soc. Mass Spectrom. **4**, 616 (1993).
[8] Y.-L. Chen, B. A. Collings, and D. J. Douglas, J. Am. Soc. Mass Spectrom. **8**, 681 (1997).
[9] J. H. Whealton and S.-B. Woo, Phys. Rev. A **6**, 2319 (1972).
[10] L. A. Viehland and A. S. Dickinson, Chem. Phys. **193**, 255 (1995).
[11] R. Baranowski and M. Thachuk, J. Chem. Phys. **111**, 10061 (1999).
[12] R. Baranowski, B. Wagner, and M. Thachuk, J. Chem. Phys. **114**, 6662 (2001).
[13] R. Baranowski and M. Thachuk, Phys. Rev. A **63**, 032503 (2001).
[14] R. Baranowski and M. Thachuk, Phys. Rev. A **64**, 062713 (2001).
[15] H. Goldstein, *Classical Mechanics*, 2nd ed. (Addison-Wesley, Don Mills, Canada, 1981).
[16] X. Chen and M. Thachuk, Int. J. Quantum Chem. **101**, 1 (2005).
[17] S. D. Augustin and W. H. Miller, J. Chem. Phys. **61**, 3155 (1974).
[18] S. D. Augustin and H. Rabitz, J. Chem. Phys. **71**, 4956 (1979).
[19] R. Baranowski and M. Thachuk, J. Chem. Phys. **110**, 11383 (1999).
[20] L. A. Viehland, Chem. Phys. **101**, 1 (1986).